# Analyzing the Stress and Modal Behavior of a Reconfigurable Gripper's Finger with Different Fabrication Materials

Ahmed Khalid Ahmed*
Electrical Engineering Department, Salahadin University-Erbil, ERBIL, IRAQ, ERBIL, 44001, Kurdistan, Iraq
Email: ahmad.ahmed@su.edu.krd

Safeen Yaseen Ezdeen
Mechanical Engineering Department, Salahadin University-Erbil, ERBIL, 44001, Kurdistan, Iraq
Email: Safeen.ezdeen@su.edu.krd

Ahmad Mohamad Sinjari
Electrical Engineering Department, Salahadin University-Erbil, ERBIL, IRAQ, ERBIL, 44001, Kurdistan, Iraq
Email: Ahmad.Sinjari@su.edu.krd

***Abstract*—A novel and new reconfigurable gripper was designed, conceptualized, and demonstrated in the previous study. The new gripper comprises six modular fingers that can rotate and clamp simultaneously. The finger assembly consists of two links, the finger arm, and the finger base. During grasping the desired object, the finger arm is in contact directly with the object. Thus, the Finger arm will be subjected to Stress and Modal analysis experiments using Fusion 360 CAD, CAM, and CAE software in this study. Moreover, to fabricate a prototype of the new gripper, the materials used in gripper fabrication are derived from studies conducted around gripper fabrication. In the simulation environment, eight materials were selected, and each material was simulated on the Finger arm. There are two major categories of materials: rigid and solid materials (Aluminum Alloy 2024-T351, Titanium Alloy 6Al-4V, Stainless Steel, Nickel-Copper Alloy 400). Another group of materials used in 3D printing is thermoplastic materials (ABS, PLA, Nylon, and Plastic). A Stress-Strain curve was plotted using ANSYS 2020 simulation software to examine the plasticity and elasticity of the first material group. Simulation results were presented as tables and in graphical form. Afterward, mechanical properties were compared. According to the results, Titanium is the most robust material in the first group of materials, followed by Steel. Compared to the other materials, Aluminum is ranked; third, while Nickel shows very little strength. In addition, PLA and Nylon are the most robust materials, with a load capacity of 8kg and higher safety factors than the target. Plastic, by comparison, can stand 3kg, while ABS is the most fragile, being able to hold only 2kg.**

***Index Terms*—Reconfigurable gripper, Stress-Strain curves, Modal Analysis, Stress Analysis, Gripper fabrication materials, fusion 360, ANSYS, FEM**

## I. Introduction

For fabricating the new gripper demonstrated in the previous study, it is necessary to perform all the steps from the design to the manufacturing. The first step is the design of the mechanisms and the concepts using CAD software. The new gripper has six modular fingers operated by electric motors.

In addition, the gripper is powered by six motors; one motor rotates each finger separately, and another provides clamping force. An overview of the newly designed reconfigurable gripper is shown in Fig. 1. The gripper can be arranged into different finger configurations depending on the object's geometry and shape.

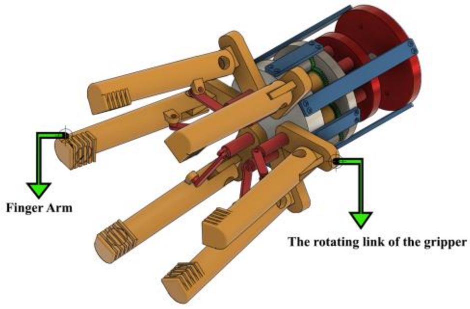


Figure 1. The new modular gripper assembly

A total of six motors can be used to adjust the fingers. Additionally, the main finger assembly consists of two links and one joint mechanism with two degrees of freedom. Therefore, the gripper has twelve degrees of freedom (12 DOF) and six fingers. Fig. 2 demonstrates the modularity of the gripper design by constructing a different number of fingers. The gripper has one configuration for three-finger and six-finger, while it has three configurations for four and five fingers [1].

Another essential step in designing a product is testing the design capability and material selection process using simulation software before fabrication. For this purpose, the simulation software Fusion 360 and ANSYS 2020 are used to test the new gripper capability. The ability of the gripper to withstand forces exerted on the gripper parts during grasping is crucial.

Manuscript received July 13, 2022; revised September 29, 2022.


doi: 10.18178/ijmerr.11.11.820-833

The materials used in fabricating the robotic grippers are generally Aluminum, Titanium, Steel, Nickel, ABS, PLA, Nylon, and Plastic. In the gripper design process, researchers have widely covered this topic regarding material selection. As a result, the materials mentioned above are used for gripper fabrication.

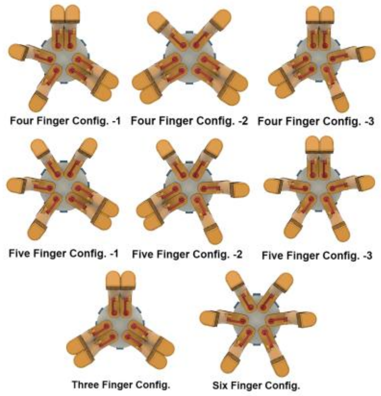


Figure 2. Gripper modularity testing by constructing a different number of fingers

For example, Steel and Aluminum are essential materials used in gripper design and analysis in [2]. Also, the gripper was fabricated using Steel Alloy in [3].

Similarly, the gripper prototype in [4] is manufactured using 3D printing technology with ABS plastic because ABS is a strong, durable production-grade thermoplastic used in many industrial products. Further, the work-piece material is selected as Aluminum Alloy AL2014 in [5]. Also, the gripper parts were fabricated from Structural Steel in [6]. Moreover, the two-fingered robot gripper's material was low Carbon Steel (AISI 1015 HR) in [7]. Steel, Cast Iron, Titanium, and Aluminum are the most used materials for the manipulator robot parts, as mentioned in [8]. However, it is also declared in [9] that the most used materials for 3D printing are ABS and PLA, and the use of Nylon is increasing considerably. Furthermore, it also endorsed that PLA is used for the gripper design as mentioned in [10]. Similarly, Steel was the selected material for the slide O-Cam mechanism robot gripper in reference [11].

Generally, material selection for gripper designs is as follows: if the weight is primacy, then Aluminum is the proper material. On the other hand, if the corrosion opposition is under discussion, Steel can be the material for the gripper design. Finally, if the temperatures are the working issue, Nickel can be selected. Also, when the lightness of the gripper is preferred, a lightweight material should be chosen, such as Steel [12]. In addition, two different materials were used in [13], Steel Alloy and Titanium, for five fingered robotic gripper materials and cost analysis. Another material used for gripper design is Teflon. For example, in the design of the mechanical gripper of Aristo Robot for Welding.

For this study, we analyze and test the gripper's primary component that will be subjected to a force during the grasping process. The central part of the gripper, which can be essential to experiment, is the Finger arm or the first link of the finger assembly. This component will be directly in contact with the objects that the gripper will grasp.

## II. Materials and Methods

Two simulation tools will be used for this study, Fusion 360 and ANSYS 2020. A total of eight materials were selected in the simulation environment. These materials are of two groups; the first group is metal and rigid materials such as (Aluminum Alloy 2024-T351, Titanium Alloy 6Al-4V, Stainless Steel, and Nickel-Copper Alloy 400). Moreover, the second group is the materials used in additive manufacturing, such as (ABS, PLA, Nylon, and Plastic).

For both groups of materials mentioned above, we designed experiments to test the finger arm for each material. Stress and Modal analysis will be conducted for the first and second groups of materials. The results will be recorded in tables, and then some significant results as graphics will be demonstrated. Stress-Strain curves will be plotted for the first group of materials as they have elasticity and plasticity properties, and the second group of materials has only elasticity.

For the rigid materials in the first group, two forces should be specified for the experiment to work correctly; the first force, denoted by Force 1, is applied from 2N up to 2500N. Nevertheless, the second force denoted by Force 2 is selected to be from 2N up to 350N. Fig. 1 shows the two forces and their positions. The 2 Newton force value was chosen as the software does not take zero value forces to start the experiment from zero. Moreover, the Force 1 and Force 2 values will be from 10N for the second group of materials up to 150N. After inserting the force values into the software, the next step is to apply the boundary conditions.

In the simulation process, the environment of simulations should be studied carefully to be as close as possible to the reality of the actual mechanism. The new gripper's forces are distributed along with the fingertips and the pin slot, connecting the finger arm with the actuation link. The distribution of the forces is illustrated in Fig. 3. Force 1 is the force along with the fingertip of the gripper, and Force 2 is which actuates the fingers.

Regarding boundary conditions, each finger arm should be constrained from the two pin-slots, the first pin-slot (the first constraint) connects the finger arm with the second link of the finger assembly, and the second pin-slot (the second constraint) connects the finger arm with the first actuation link. The loads and boundary conditions should be applied before getting the simulation results. The process of applying the boundary conditions is shown in Fig. 4.

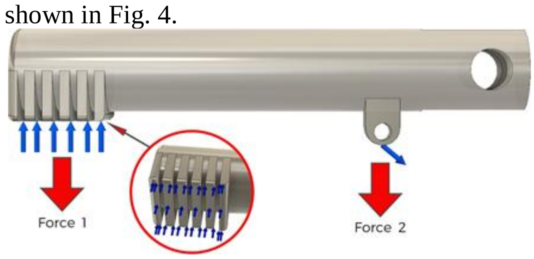


Figure 3. Distribution of forces.


Figure 4. Constraints were applied to the Finger arm.

The final step is meshing, which should be applied before starting the simulations and getting the results. The FEM concept is based on splitting the domain into a discrete number of elements to calculate the results. Therefore, meshing aims to obtain accurate results from the FEM. However, the results achieved from the FEM are an approximation to the actual calculations. Thus, the default meshing setting in FUSION 360 will be used for the current gripper design, and results will be obtained using the built-in mesh setting of the simulation software. In Fig. 5, the mesh number of elements and nodes are presented.

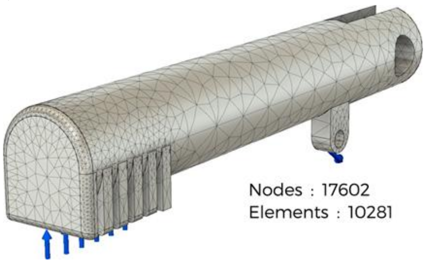


Figure 5. Meshing process after generating the elements and nodes.

Moreover, the mesh setting and parameters will remain the same for all the materials tested in this study. Therefore, the mesh parameters and setting will not be altered for the static stress and modal analysis.

Once the meshing process is applied, the simulation can be started by clicking the solve button. The results obtained from these simulations are stresses, strains, displacements, safety factors, and modal frequencies.

Stresses and Strains are essential to be studied because when two bodies are in contact (the fingertip and the object's surface are intended to be grasped) due to the material properties, the contact along the line changes to contact along the surface. Also, the stresses and strains developed in the two bodies will be three-dimensional. Moreover, if the stresses are not under control, they can cause failures such as cracks, pits, and flaking on the material's surface [11].

Further, when evaluating the strength of any machine, the first step in the design/analysis of machine components is generally static stress analysis [2].

Stress analysis is a discipline that uses various methods to determine the stresses and strains induced in the materials and structures exerted by forces. As a result of stress analysis, we can understand and describe the force distribution throughout the structure and each component. When the forces vary with time, the Stresses, Strain, and deformations are also time functions. Furthermore, the Stress analysis is performed in mathematical calculation and the Finite Element Method. Mathematically, the process is complicated because too many parameters should be known before the calculation process. So the second option is preferable to using simulation software as mentioned in [8].

In the following sections, the materials typically used in gripper fabrication will be tested for static stress analysis, and later modal analysis will be conducted. The mechanical properties of the materials selected in simulation software to be used in the gripper fabrication are shown in Table I.

These simulations will be demonstrated in tables and graphics in the results section. It is imperative to mention that the lower target of the safety factor is set to be three by default. This target value can be changed to any number that fits the standard of any project. For this study, the default target will remain at three.

Besides, there are three critical statuses during the simulation. The Normal Status is the first record in Table II. It occurs when the design is over-engineered and can withstand the applied force. Marginal Status is the second record in Table II. If the design is marginal, it may be sufficient, but outside factors may cause it to bend or break. Finally, the last Status is when the design cannot withstand the force and will permanently break or bend, for example, the third record in Table II.

The third Status will not be applicable in some cases, especially when the material is strong and will not break under the applied forces. Since they do not affect the material's mechanical behavior, we will not show the initial values when it can withstand the forces. Therefore, only one record will be shown before the status change to marginal.

Moreover, the software calculates Probe points' minimum and Maximum safety factors areas on the design. The Probe points show the Min. Safety factor and Max. Safety factor on the element under the test. The simulation results for forces will be shown graphically to compare the different materials used in gripper fabrication. In addition, one graphical result will be shown for the normal Status, one for marginal Status, and one for break or bend status.

## III. Simulation Results

From the simulation results of Aluminum material shown in Table II, it can be seen that when the applied forces are small, the safety factor is very high examples are the safety factors for (2 N up to 400 N) for Force-1 and (2 N up to 200N) for Force-2, in Aluminum Alloy 2024-T351 Table II (A).

The safety factor is between 15 and 3.1220. This safety factor shows that the design is over-engineered at these forces, and the element under the test can withstand the forces applied. On the other hand, when the forces are increased, the safety factor will drop accordingly, and its value is between 2.7640 and 0.4871 for the rest of the force values applied.

For Aluminum, the Safety factor results show that when the value is more significant and equal to three, the design is expected not to break or bend. However, when the Safety factor is below three, for example, 1.55, the design is marginal and may be sufficient, but outside factors could cause it to bend or break. In some cases, when the Safety Factor is 0.82 or less, the design is now expected to break or bend permanently under the current analysis criteria.

Calculating displacement or deflection of the finger arm under different applied forces is crucial.

TABLE I. THE MECHANICAL PROPERTIES OF THE MATERIALS USED IN GRIPPER FABRICATION.

| Properties | Aluminum | Titanium | Steel | Nickel | ABS | PLA | Nylon | Plastic |
|---|---|---|---|---|---|---|---|---|
| Young's Modulus | 73.080 GPa | 113.770 GPa | 200.000 GPa | 179.300 GPa | 2.240 GPa | 1.280 GPa | 2.758 GPa | 0.709 GPa |
| Poisson's Ratio | 0.33 | 0.34 | 0.29 | 0.32 | 0.38 | 0.36 | 0.35 | 0.40 |
| Shear Modulus | 27473.68 MPa | 42451.49 MPa | 77519.38 MPa | 65000 MPa | 805 MPa | 1287 MPa | 1000 MPa | 750.000 MPa |
| Density | 2.78 g/cm ³ | 4.43 g/cm ³ | 7.85 g/cm ³ | 8.83 g/cm ³ | 1.06 g/cm ³ | 1.25 g/cm ³ | 1.12g/cm ³ | 1.29 g/cm ³ |
| Yield Strength | 324.05 MPa | 882.52 MPa | 344.73 MPa | 220 MPa | 20. MPa | 70. MPa | 70.4 MPa | 30 MPa |
| Tensile Strength | 468.84 MPa | 951.47 MPa | 448.15 MPa | 558 MPa | 29.6 MPa | 59 MPa | 75.7 MPa | 40 MPa |

TABLE II. THE RESULTS OBTAINED FROM STATIC STRESS ANALYSIS FOR THE MATERIALS USED IN GRIPPER FABRICATION.

| No. | Force 1 (N) | Force 2 (N) | Safety Factor Min. | Max. Stress (MPa) | Max Strain | Kg |
|---|---|---|---|---|---|---|
| A- | Static Stress Analysis for Aluminum | | | | | |
| 1 | 400 | 200 | 3.1220 | 103.80 | 0.00221800 | 40.78719 |
| 2 | 800 | 300 | 1.5470 | 209.40 | 0.00447900 | 81.57439 |
| 3 | 1500 | 350 | 0.8171 | 396.60 | 0.00849000 | 152.952 |
| B- | Static Stress Analysis for Titanium Alloy 6Al-4V | | | | | |
| 1 | 1000 | 300 | 3.3650 | 262.3 | 0.003638 | 101.968 |
| 2 | 1500 | 350 | 2.2330 | 395.3 | 0.005484 | 152.952 |
| 3 | 2500 | 350 | 1.3310 | 663 | 0.009204 | 254.92 |
| C- | Static Stress Analysis for Stainless Steel | | | | | |
| 1 | 400 | 200 | 3.289 | 104.8 | 0.00079 | 40.78719 |
| 2 | 1000 | 300 | 1.297 | 265.8 | 0.002006 | 101.968 |
| 3 | 1500 | 350 | 0.8606 | 400.6 | 0.003025 | 152.952 |
| D- | Static Stress Analysis for Nickel-Copper Alloy 400 | | | | | |
| 1 | 200 | 150 | 4.234 | 51.96 | 0.0004407 | 20.3936 |
| 2 | 800 | 300 | 1.047 | 210 | 0.001815 | 81.57439 |
| 3 | 1000 | 300 | 0.8335 | 263.9 | 0.002282 | 101.968 |
| E- | Static Stress Analysis for ABS Material | | | | | |
| 1 | 20 | 20 | 3.841 | 5.207 | 0.003571 | 2.039 |
| 2 | 70 | 70 | 1.097 | 18.22 | 0.0125 | 7.138 |
| 3 | 80 | 80 | 0.9602 | 20.83 | 0.01429 | 8.157 |
| F- | Static Stress Analysis for PLA Material | | | | | |
| 1 | 80 | 80 | 3.356 | 20.86 | 0.02477 | 8.157 |
| 2 | 90 | 90 | 2.983 | 23.47 | 0.02787 | 9.177 |
| 3 | 150 | 150 | 1.79 | 39.11 | 0.04645 | 15.295 |
| G- | Static Stress Analysis for Nylon Material | | | | | |
| 1 | 80 | 80 | 3.372 | 20.88 | 0.01144 | 8.157 |
| 2 | 90 | 90 | 2.998 | 23.49 | 0.01287 | 9.177 |
| 3 | 150 | 150 | 1.799 | 39.14 | 0.02144 | 15.295 |
| H- | Static Stress Analysis for Plastic Material | | | | | |
| 1 | 30 | 30 | 3.845 | 7.801 | 0.01704 | 3.059 |
| 2 | 40 | 40 | 2.884 | 10.4 | 0.02273 | 4.078 |
| 3 | 120 | 120 | 0.9614 | 31.21 | 0.06818 | 12.236 |

It shows the positions when Minimum and Maximum deflections will occur on the design. The displacement will increase when the force applied increases. The minimum displacement is 0.1642 mm, and the maximum is 1.026 mm. The Finger arm design is marginal at (1000 N, 300 N) force values. The breaking or permanent bending will occur when (1500 N, 350 N) forces are applied, and the displacement is 0.6158 mm.

The design can withstand stresses up to (800 N, 300 N) forces at which the design reaches the marginal situation. After that, the stresses will appear for (1500 N, 350 N) forces, making the design bend permanently or break.

The Strain will increase as the force applied increases. The Strain (equivalent) for the selected forces is between 0.002218 and 0.01425. The Max. Stress and Max. Strain mainly occurs around the area where the second pin slot is located. Therefore, the design in this area can be improved to improve the overall design. In Fig. 6, the Max. Von Mises Stresses for the selected Forces and the Max. Strains (Equivalent) are shown.

The simulation software can also calculate the Normal and Shear stresses and strains. Nevertheless, unfortunately, FUSION 360 cannot plot Stress-Strain curves, which is essential in understanding the Elasticity and Plasticity of the current design and materials. For that reason, it is necessary to switch to the ANSYS R20 simulation software and conduct structural analysis to get Stress-Strain diagrams for the selected forces mentioned earlier. Therefore, the Stress-Strain curves will be shown in the last section of this study.

For the Titanium Alloy 6Al-4V, different force magnitudes were applied to the finger arm to obtain the static stress analysis results. The static stress analysis for the Titanium Alloy is shown in Table II (B).

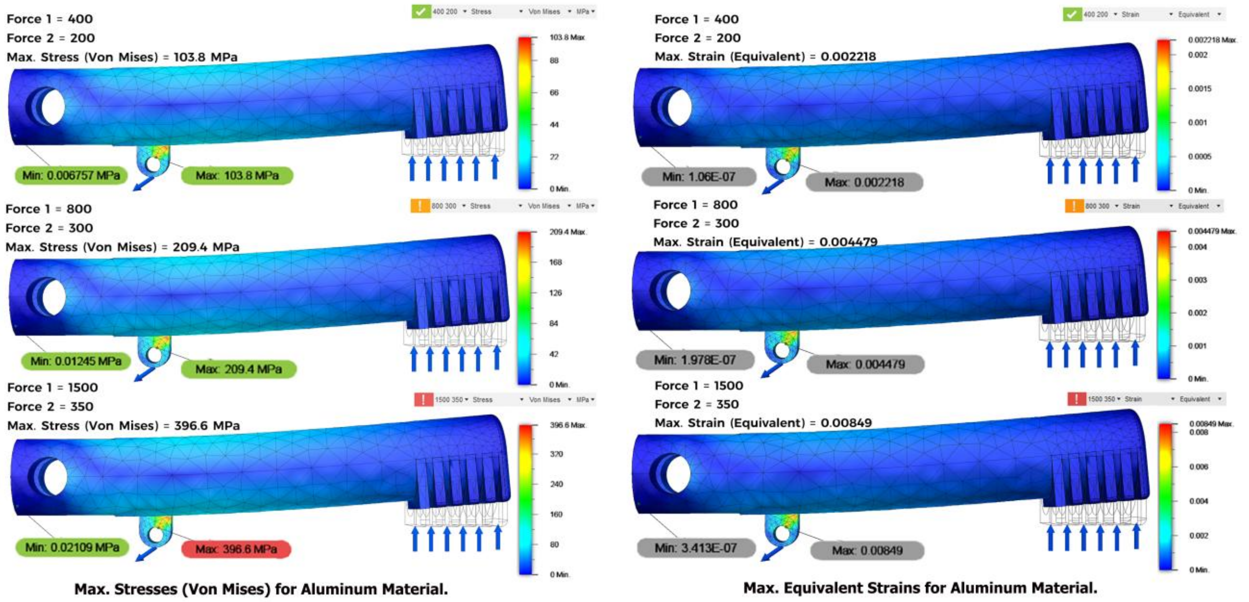


Figure 6. Maximum stress and strains for aluminum material

Unlike Aluminum, The safety factor for Titanium will remain higher, and it is between 15 and 3.3650 (above the target point) even for higher forces. These safety factors indicate that the design is over-engineered at these forces, and the element under the test can withstand the forces applied.

It is clear from the table that the safety factor decrease when the force applied increases, but it is not dropping like Aluminum to make the design break or bend for the selected forces in the table. The safety factor in the table shows that the material is strong and can withstand higher forces.

The maximum displacement for Titanium material is between (0.0005267 mm) and (0.6590 mm). Besides, the Von Mises stresses are slightly higher than the Aluminum material, but the strain values of Titanium show higher values than Aluminum. Moreover, the maximum stresses and strains are shown graphically in Fig. 7.

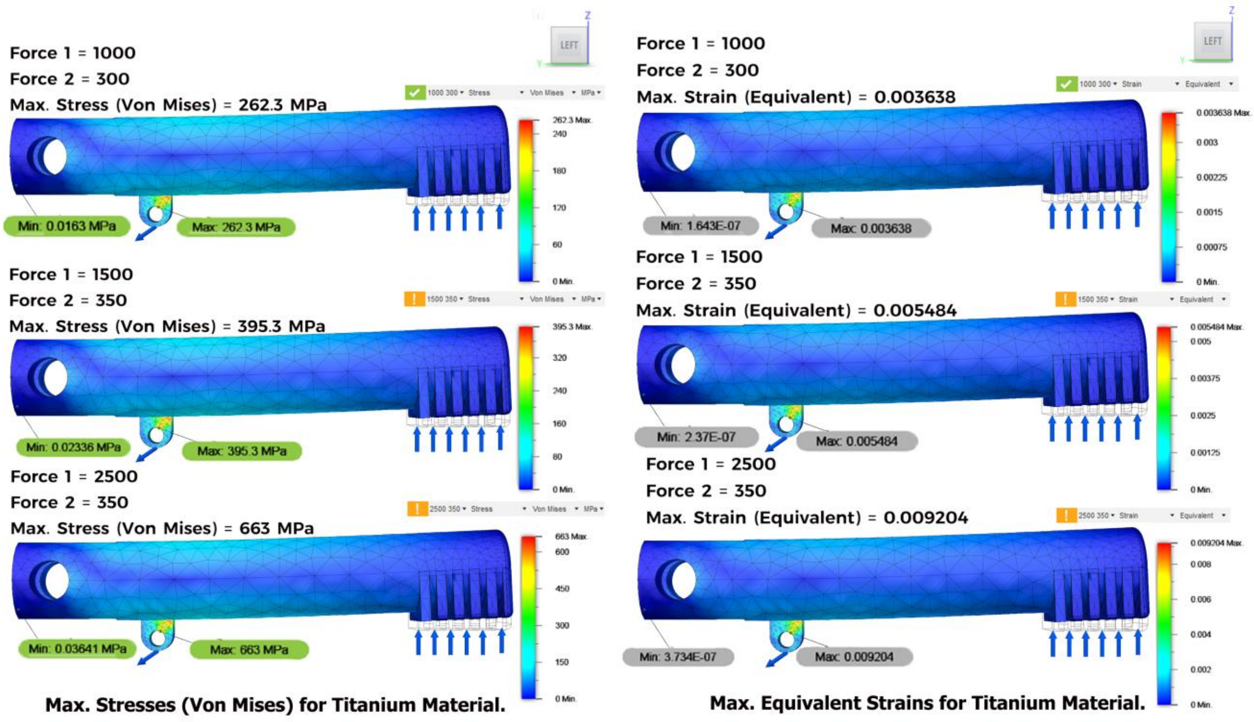


Figure 7. Maximum stresses and strains for titanium material.

For the Stainless Steel material, the results of Static Stress Analysis were collected and tabulated in Table II (C). The Safety Factor values are high for the small forces, and they will decrease when the force is increased. If the safety factor is above the target value for the forces between 2 N and 400 N, then the safety factor will drop below the target value. The design will remain marginal until the 1500 N force is applied; the design will permanently break or bend.

Stainless Steel is very similar to Aluminum Material because the Static Stress tables for both materials are slightly different. The safety factor of both are above the target value for the forces smaller than 450 N, and the design will be marginal between 450 N and 1000 N forces. Further, the design for both materials will break or bend permanently for forces above 1000 N. On the other hand, Titanium is more substantial than Aluminum and Stainless Steel.

The displacements for Stainless Steel are between 0.0003003 mm and 0.3756 mm. The Stresses are between 0.525 MPa and 672 MPa. Moreover, the Strains (Equivalent) are between 0.000003793 and 0.005078. Stresses (Von Mises) and Strain values for different forces graphically are shown in Fig. 8.

So far, Titanium material is the most robust material, and it shows acceptable results even in very high forces compared to Aluminum and Stainless Steel.

For the Nickel-Copper Alloy 400 material, the static stress analysis is shown in Table II (D). This material is weaker mechanically as the safety factor drops after the target value at 300 N force compared with the preceding materials. Therefore, the design will be marginal between 250 N and 1000 N forces, and the design will break or bend permanently when the 1000 N force is exceeded.

The graphical results obtained from the simulations are shown in Fig. 9.

The static stress analysis for the materials used in 3D printing is performed below. First, the tests were conducted on ABS (Acrylonitrile butadiene styrene) material, followed by PLA, Nylon, and Plastic. The results of simulations for ABS are tabulated in Table II (E).

It can be seen that ABS can withstand 20 N of force without breaking or bending as the safety factor is above the target value. When the force exceeds 20 N, the safety factor drops below the target value, but still, the design is marginal. Moreover, when the force is 80 N, the finger arm will break or bend permanently.

The displacement for 10 N force is 0.1334 mm, which starts to increase until it reaches 1.067 mm when the finger arm breaks or bends permanently. When the design breaks, the stresses, and Strain are 20.83 MPa and 0.01429, respectively. The graphical results are shown in Fig. 10.

PLA material and the mechanical properties were manually inserted into the FUSION 360 software as the material does not exist in the default library. Polylactic Acid (PLA) simulation results are listed in Table II (F). PLA and ABS are thermoplastics, but the table shows that PLA is more vital and stiffer than ABS.

In addition, the safety factor is very high at 20 N force compared to ABS. For example, when ABS breaks at 80 N force, the safety factor of PLA is above the target value (3.356).

So it is clear that more than 150 N should be applied to break the finger arm in the case of PLA material. The graphical results are shown in Fig. 11.

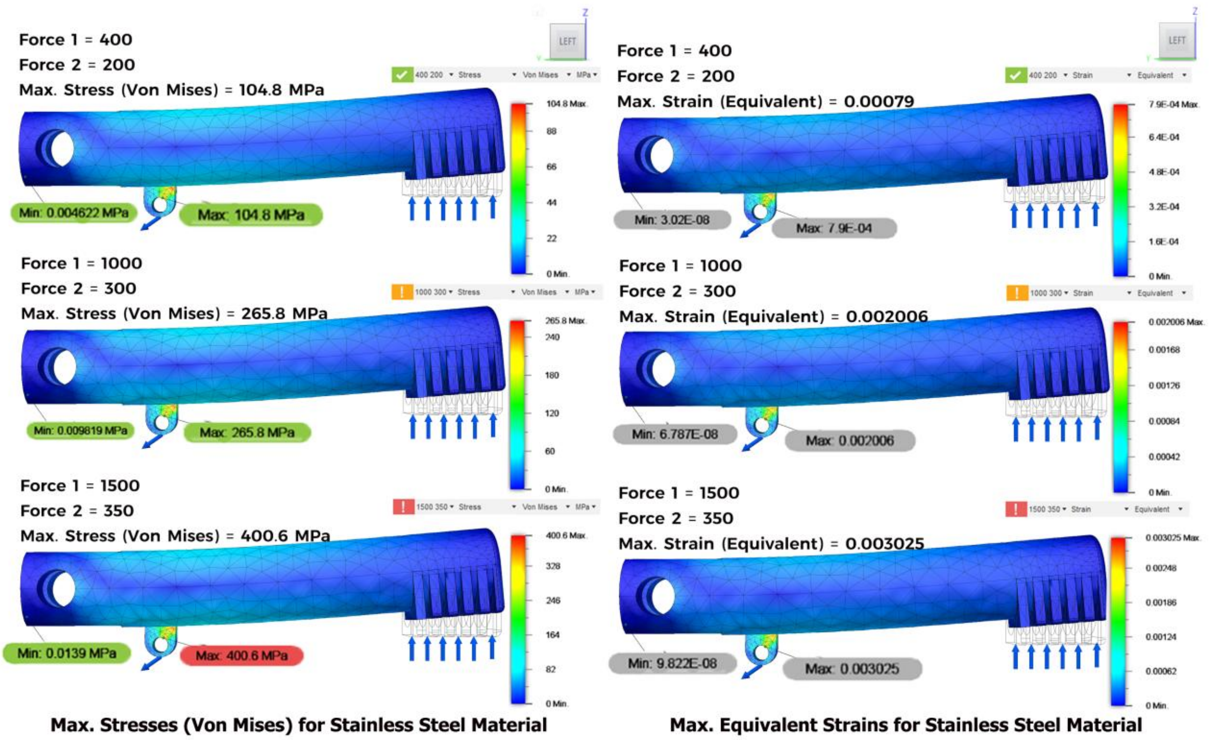


Figure 8. Maximum stresses and strains for stainless steel material

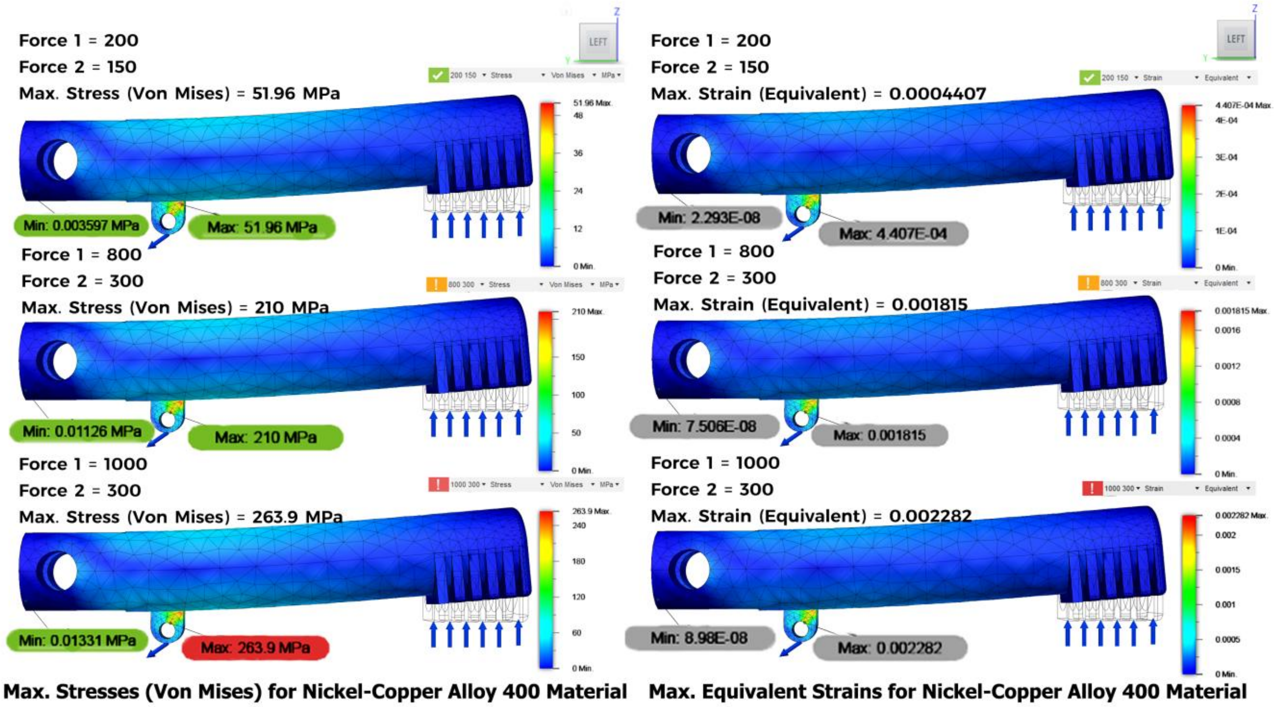


Figure 9. Maximum stresses and strains for Nickel-copper alloy 400 material.

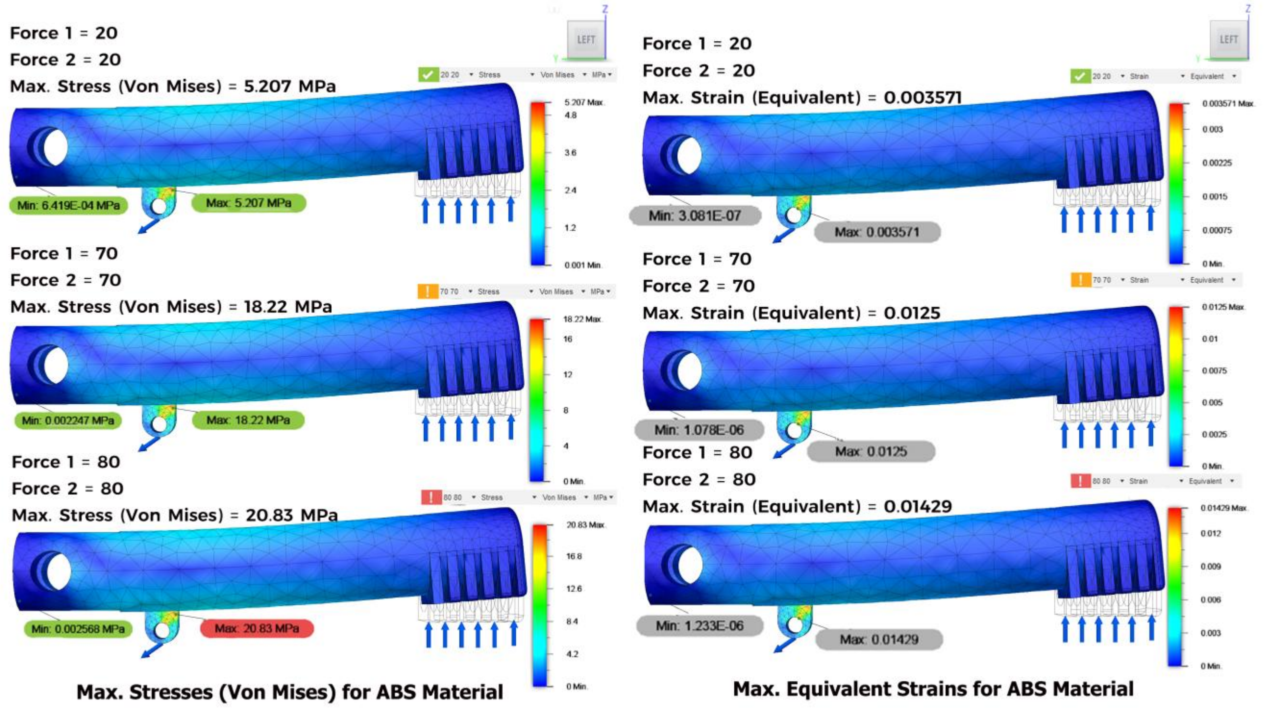


Figure 10. Maximum stresses and strains for ABS Material.

Another material that is used widely in 3D printing is Nylon. The simulation results of Nylon material are shown in Table II (G).

The results obtained from the simulations are slightly different from those obtained for PLA material. However, according to the results, Nylon is also more solid and stiffer than ABS material. The graphical results are shown in Fig. 12.

Finally, the last material analyzed for the static stress test is Plastic. The simulation results are shown in Table II (H). The safety factor of Plastic remains above the target value when 30 N forces are applied.

However, when the forces exceed 30 N, the safety factor drops below the target value, but the prototype design is still marginal at the current analysis criteria. The finger arm will break or bend when 120 N forces are applied. The graphical results are shown in Fig. 13.

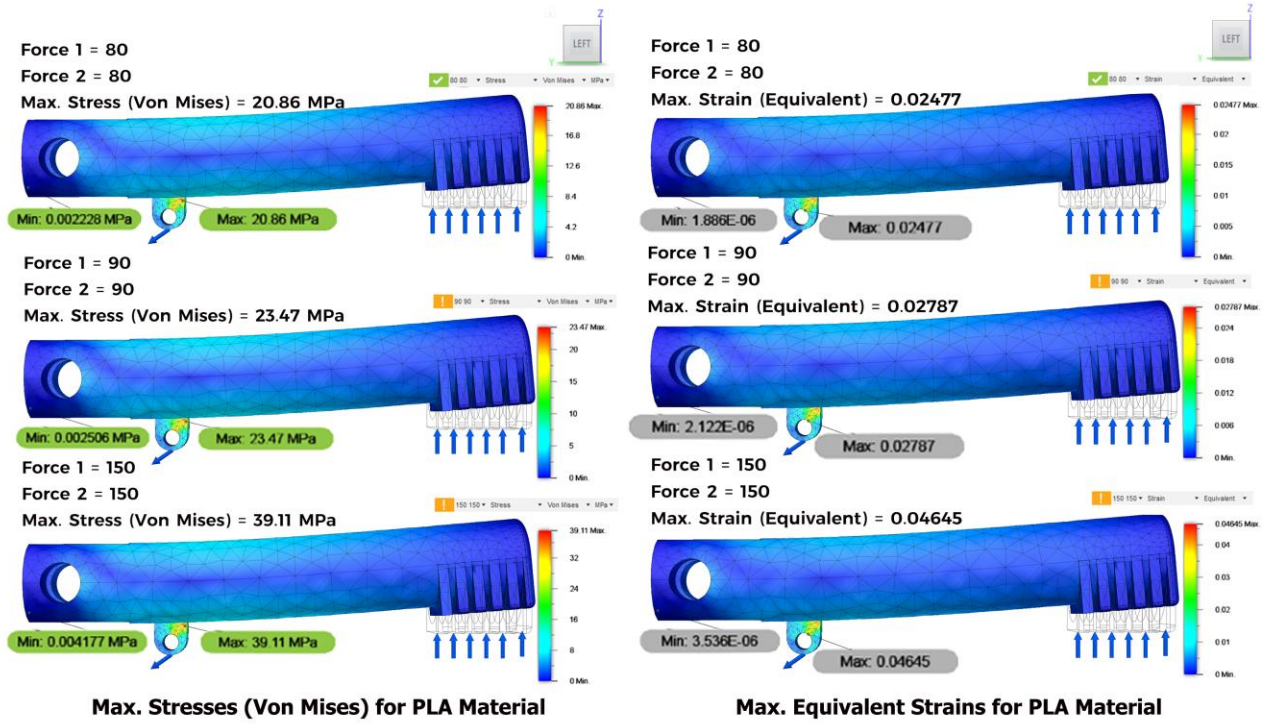


Figure 11. Maximum stresses and strains for PLA material

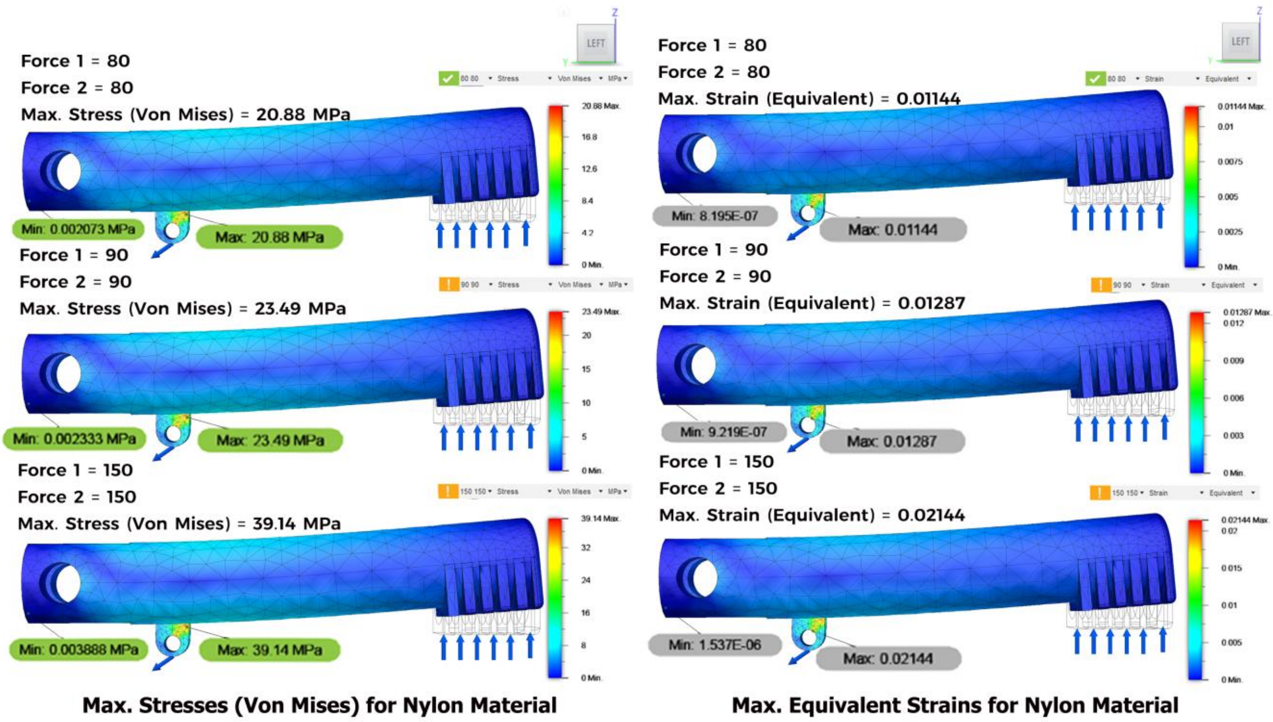


Figure 12. Maximum stresses and strains for Nylon material.

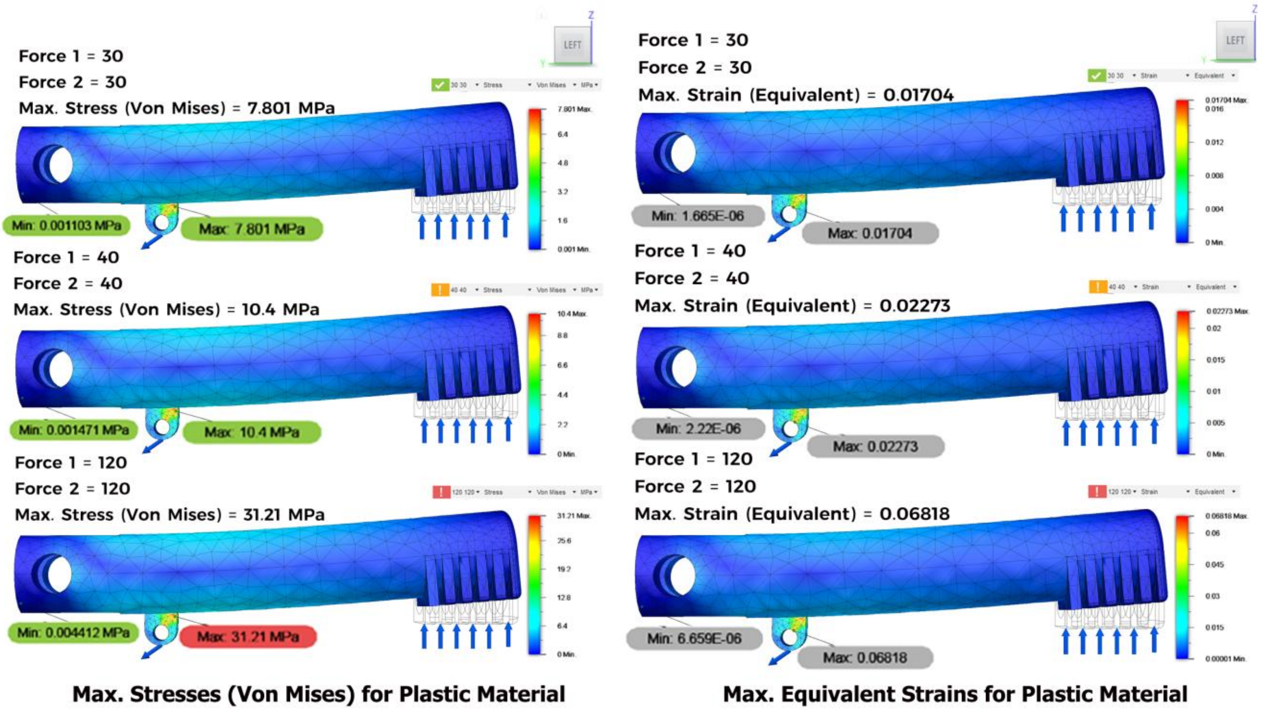


Figure 13. Maximum stresses and strains for plastic material.

## IV. Stress-Strain Curves

Stress and Strain are the basic concepts used to describe how a body reacts to external loads. Stress can be defined as the quantity that describes the distribution of internal forces due to externally applied loads within the body. Stress can also be defined as the internal force measurement per unit area. In contrast, Strain is defined as a quantity describing the body's deformations due to external forces.

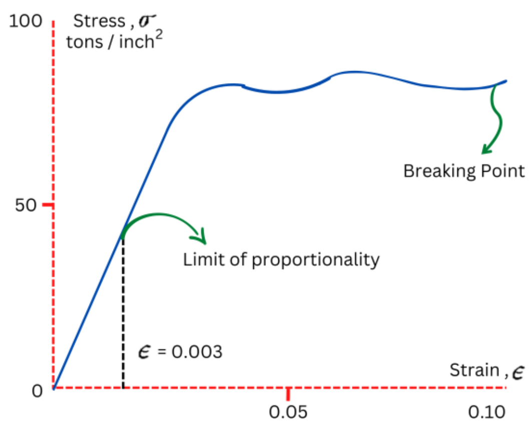


Figure 14. Stress-Strain curve for high-strength steel material.

However, the concept of stress and Strain are closely linked, and the relation between the two quantities can be described using a stress-strain curve. The stress-strain curve is different for different materials. For instance, the stress-strain curve of high-strength Steel has the form shown in Fig. 14.

High-tensile Steel shows a linear stress-strain curve for stresses up to about 50 tons/in$^2$. Within this range, Hooke's Law is obeyed. The material is also elastic in this range, and no permanent extensions are left over after removing the stresses.

Therefore, when the stress-strain curve is linear, this range is called the Elastic region. Steel typically has a stress-strain ratio of 13,000 tons/ in2 for this linear region; this ratio is known as Young's modulus and is denoted by E.

The Stresses that exceed the linear-elastic range lead to a nonlinear increase in strains. Furthermore, removing stress leaves the material with some permanent extension; this range becomes nonlinear and non-elastic. The nonlinear range is called the Plastic region [14].

This study will demonstrate the stress-strain curves for all the previously mentioned materials used in gripper fabrication. Fig. 15 shows the strain-stress curves for Aluminum, Steel, Titanium, and Nickel.

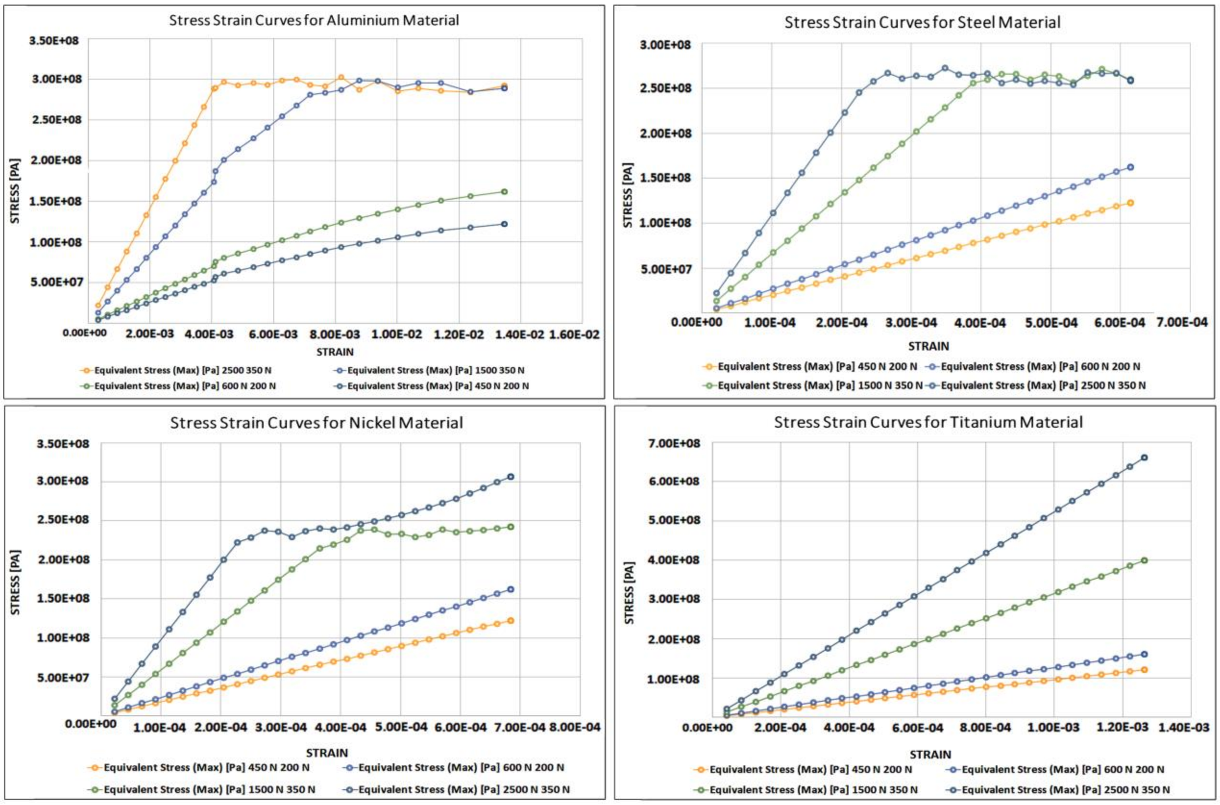


Figure 15. Stress-Strain Curves for Aluminum, Titanium, Stainless Steel, and Nickel.

## V. Modal Frequency Analysis

Modal analysis is a numerical method for calculating structural vibration properties. Further, structural vibration properties include natural frequency and mode shape. Therefore, modal analysis is the most fundamental dynamic analysis and the basis of other dynamic analyses [15].

The modal analysis is used to determine the natural frequency and mode shapes of the finger arm of the gripper design. In addition, the modal analysis determines the vibration characteristics of mechanical components or the structure, namely the structure's natural frequency and the vibration mode, which are essential parameters for dynamic loads. When a mechanical system performs a modal analysis, parts and components with noticeable vibrations can be identified. If a weak link is identified, sensible improvements can be proposed to avoid resonance [16].

Most structures can be brought into resonance. Under suitable conditions, a structure can be vibrated with excessive sustained vibratory motion. Resonance vibrations are caused by an interaction between the inertial and elastic properties of the materials within a structure. Further, one of the most valuable methods of understanding resonance vibrations is the principle of trapped energy. When energy enters a structure due to dynamic loads of any kind, resonance vibrations occur when the energy is trapped within the structure's boundaries, moves freely within these boundaries, and cannot easily escape. This trapped energy manifests itself in traveling waves of deformation, which are also assigned a characteristic frequency. Waves moving within the structure and reflecting from its boundaries add to a standing deformation wave. This standing wave is called a mode shape, and its frequency is the structure's resonant or natural frequency [15].

Many structures were tested for performance using modal analysis; for instance, the first nine resonant mode shapes for the compliant gripper structure are presented in [17]. In the same way, through FEA performed with ANSYS, the natural frequency of the gripper based on performance evaluation and modal analysis was determined in [18]. Using the Compliant Gripper structure as an example, reference [19] demonstrated the simulation results for the first six resonant modes. A modal analysis is also conducted with ANSYS software to evaluate the dynamic performance of the mechanism.

In addition, ANSYS was used to perform a modal analysis on the Space Frame Race Car chassis. Also, five modes were demonstrated in [20] along with their natural frequencies. Further, A ten-mode shape was extracted from ANSYS simulation software in reference [21] to analyze micrograppers' modal behavior. Similarly, the modal analysis to evaluate the dynamic property of the micro-gripper was studied in reference [22]. Additionally, modal analysis was used to determine the fundamental frequencies (modes) and their associated behavior (mode shapes in [23]. To understand the dynamics of the Detachable-Jaw Robotic Gripper system, natural frequencies and mode shapes were studied in [24].

FUSION 360 simulation software was used to perform the modal frequency analysis in this study. A total of eight mode shapes were extracted from the software, and their frequencies were calculated.

It uses the finger arm structure of the gripper designed in this study to determine the frequencies and modes for each material. For example, the Aluminum Material's first natural frequency begins at 3720 Hz, and its last frequency (Mode 8) is 19526 Hz.

When Aluminum is compared with Titanium and Steel, minor differences in frequencies can be observed with the first mode frequency of 3674 Hz and the last mode frequency of 19253 Hz for Titanium. Also, the first mode frequency of 3674 Hz, and the last mode frequency of 19420 Hz for Steel material. It appears, however, that even the mode shapes are the same for the three materials. Nickel material shows lower frequencies than the three materials mentioned above. For example, the first mode frequency is 3273 Hz, but the last mode frequency is 17225 Hz, lower than Aluminum, Steel, and Titanium. However, the mode shapes remain similar for all the materials discussed. Fig. 16 shows the eight modes and their corresponding frequencies for Aluminum, Titanium, Stainless Steel, and Nickel.

A separate modal frequency analysis was conducted for ABS, PLA, Nylon, and Plastic, all 3D printing materials. ABS material has a first mode frequency of 1052 Hz and a last mode frequency of 5471 Hz. Nylon mode frequencies are similar to ABS but start at 1137 Hz and end at 5947 Hz.

On the other hand, PLA shows a lower first natural frequency starting at 732.4 Hz, and the last mode frequency is 3823 Hz. Plastic shows the lowest mode frequency at 536.3 Hz and the last at 2778 Hz. Fig. 17 shows the eight modes and their corresponding frequencies for ABS, PLA, Nylon, and Plastic.

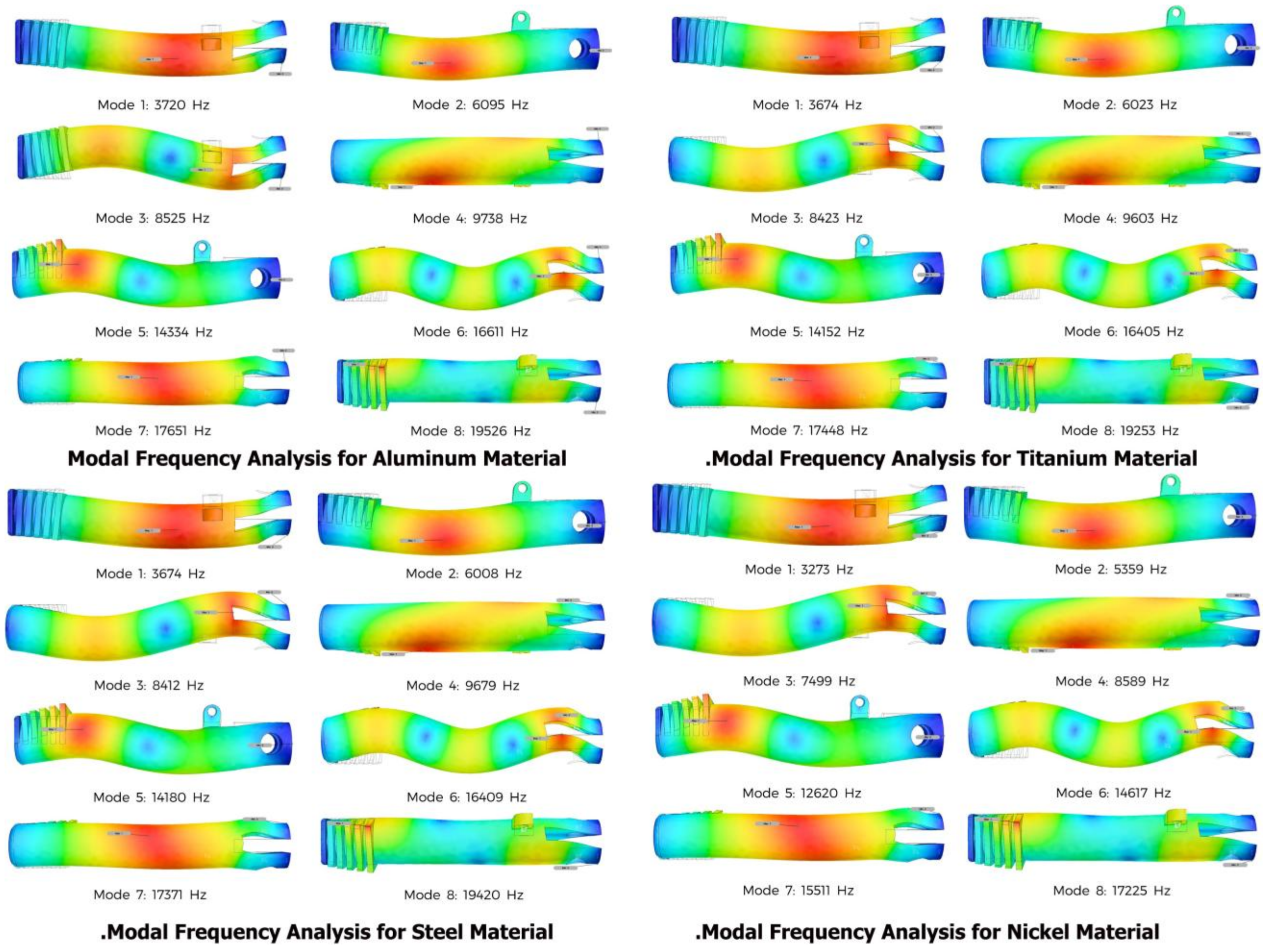


Figure 16. Modal Frequency Analysis for Aluminum, Titanium, Stainless Steel, and Nickel.

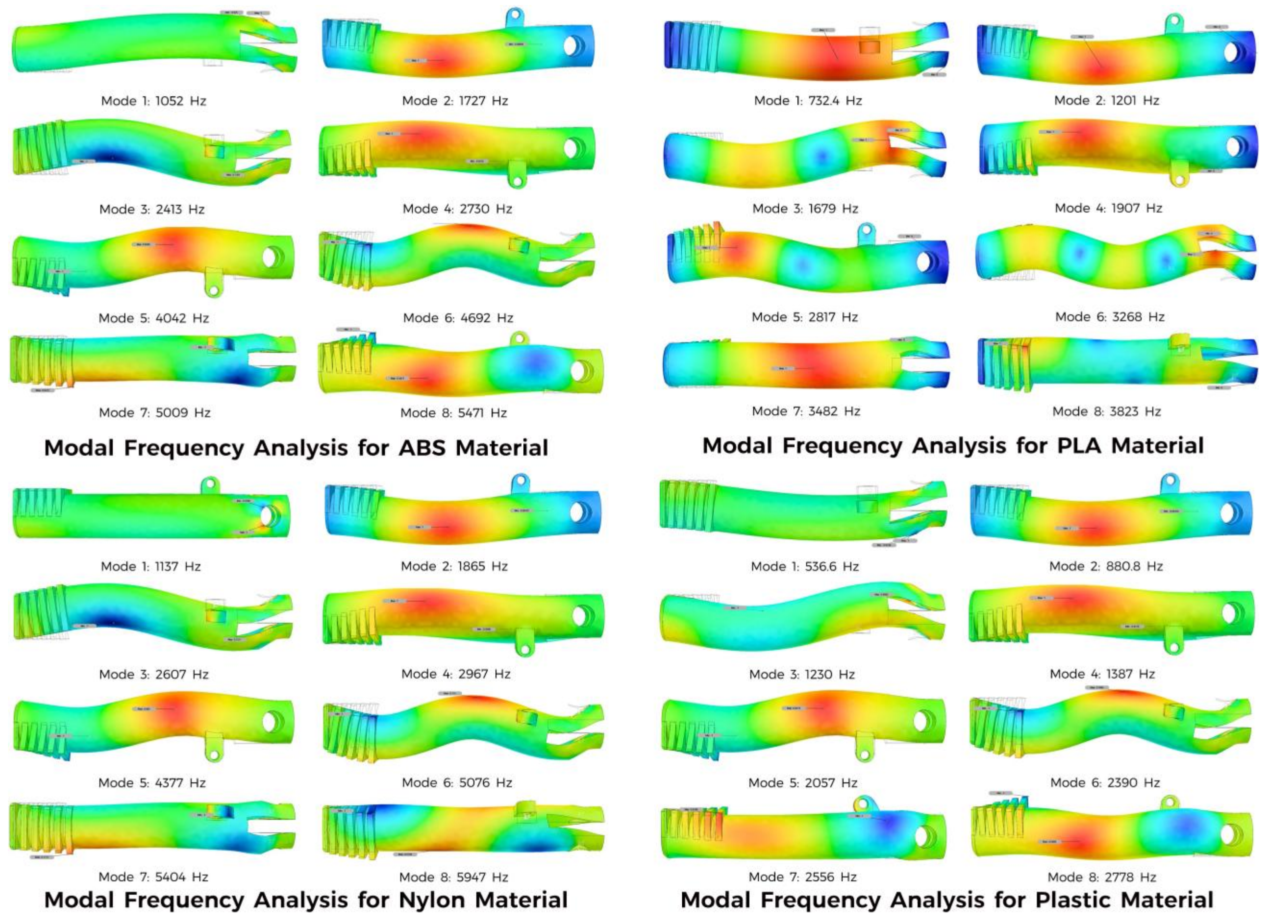


Figure 17. Modal Frequency Analysis for ABS, PLA, Nylon, and Plastic.

## VI. Discussions

For this study, the simulation results were used to understand which material will be the most substantial material by conducting Static Stress Analysis in Fusion 360. The Stress-Strain Curves were plotted to understand the Elasticity and Plasticity areas of the material.

Afterward, the Modal frequency analysis was performed to calculate the mode shapes and the critical frequencies in which the design deforms. The following tables show the comparison between the materials simulated in FUSION 360. For example, Table III shows that Titanium is a solid material compared to Aluminum, Steel, and Nickel, based on Min. Safety Factor. The Min. Safety Factor for Titanium is higher at Max. Force. The Titanium does not break or bend to the forces applied in the simulations, and it can withstand loads of more than 101 Kg.

Steel Material is in the second position and is slightly more potent than Aluminum, which comes in the third position. Nickel shows very little strength compared to other materials. Furthermore, in Table IV, the comparison is based on Maximum displacements when the Safety Factor is more significant than the target value. The Nickel material comes at the first position as its Max. Displacement is 0.04184 millimeters. In the second position, Steel with Max. Displacement of 0.06009 millimeters. Aluminum and Titanium are in the third and fourth positions, respectively.

Moreover, when the safety factor is greater than the target value, the stress in Titanium material is the highest. As a result, Steel comes after Titanium with very little difference from Aluminum.

Nickel shows minor stress when the safety factor exceeds the target value. On the other hand, Strain at Titanium is maximum, Aluminum comes at the second position, Steel comes third, and Nickel is fourth. The maximum stresses and strains when the safety factor is greater than the target value are shown in Table V. The results of thermoplastic materials are compared in Table VI. Based on the Minimum Safety Factor at Maximum Force, PLA and Nylon are the most robust materials, withstand 8 kg of load and have a safety factor higher than the target. On the other hand, Plastic can withstand three kg, while ABS is most delicate as it can resist two kg.

Furthermore, PLA bending (Max. Displacement) is maximum (1.871 mm), Plastic is second with (1.263 mm), Nylon is third, and ABS has the most negligible bending. The Maximum Displacement at Safety Factor > Target point (3) is shown in Table VII. Further, the maximum stresses and strains at Safety Factor greater than the target point (3) for the four mentioned materials are shown in Table VIII.

TABLE III. MINIMUM SAFETY FACTOR COMPARISON

| | Aluminum | Steel | Titanium | Nickel |
|---|---|---|---|---|
| Min. Safety Factor at Max. Force | 0.4871 | 0.513 | 1.3310 | 0.3297 |
| Break/Bend Point Min. Safety Factor | 0.8171 | 0.8606 | Nan | 0.8335 |
| Min. Safety Factor Before Break Point | 1.231 | 1.297 | 1.3310 | 1.047 |
| Kg at Safety Factor > Target point (3) | 40.79 | 40.79 | 101.968 | 25.49 |

TABLE IV. MAXIMUM DISPLACEMENTS AT SAFETY FACTOR > TARGET POINT (3)

| Maximum Displacements (mm) at Safety Factor > Target point | Aluminum | Steel | Titanium | Nickel |
|---|---|---|---|---|
| | 0.16420 | 0.06009 | 0.2636 | 0.04184 |

TABLE V. MAXIMUM STRESSES AND STRAINS AT SAFETY FACTOR > TARGET POINT (3)

| | Aluminum | Steel | Titanium | Nickel |
|---|---|---|---|---|
| Maximum Stresses (MPa) | 103.8 | 104.8 | 262.3 | 64.67 |
| Maximum Strains | 0.00221800 | 0.00079 | 0.003638 | 0.0005574 |

TABLE VI. MINIMUM SAFETY FACTOR COMPARISON

| | ABS | PLA | NYLON | PLASTIC |
|---|---|---|---|---|
| Min. Safety Factor at Max. Force | 0.5121 | 1.79 | 1.799 | 0.7691 |
| Min. Safety Factor at Break/Bend Point | 0.9602 | - | - | 0.9614 |
| Min. Safety Factor Before Break Point | 1.097 | - | - | 1.049 |
| Kg at Safety Factor > Target point (3) | 2.039 | 8.157 | 8.157 | 3.059 |

TABLE VII. IMUM DISPLACEMENTS AT SAFETY FACTOR > TARGET POINT (3)

| Maximum Displacements (mm) at Safety Factor > Target point | ABS | PLA | NYLON | PLASTIC |
|---|---|---|---|---|
| | 0.2669 | 1.871 | 0.8686 | 1.263 |

TABLE VIII. MAXIMUM STRESSES AND STRAINS AT SAFETY FACTOR > TARGET POINT (3)

| | ABS | PLA | NYLON | PLASTIC |
|---|---|---|---|---|
| Maximum Stresses (MPa) | 5.207 | 20.86 | 20.88 | 7.801 |
| Maximum Strains | 0.003571 | 0.02477 | 0.01144 | 0.01704 |

## VII. CONCLUSIONS

This study simulated the eight rigid type materials used in robotic gripper fabrication on the Finger arm, which is an essential part of the designed gripper. It is subjected to force during the grasping process. In terms of stiffness and vitality, Titanium far outperforms Steel, Aluminum, and Nickel, which come in second, third, and fourth, respectively. Similarly, PLA and Nylon are very robust materials, while plastics and ABS are delicate. Therefore, this study suggests fabricating the gripper with Titanium material when the gripper is intended to be used in heavy-duty applications since Titanium can withstand loads of more than 101 kilograms.

Furthermore, to demonstrate the concepts of the new reconfigurable gripper design presented in this study. A prototype gripper will be manufactured in PLA and ABS. It is possible to use these two materials to construct gripper parts with a 3D printer, and both are readily available on the market.

## CONFLICT OF INTEREST

The authors declare no conflict of interest.

## AUTHOR CONTRIBUTIONS

Ahmed Khalid Ahmed has contributed to this research by implementing the experimental and analytical work with the guidance and supervision from Prof. Safeen Yaseen and Dr. Ahmad Mohamad.

## REFERENCES

[1] A. K. Ahmed, S. Y. Ezdeen, and A. M. Sinjari, "Design of a new modular reconfigurable gripper,"*TEM J.*,vol. 11, no. 2,pp. 763–771, May 2022.

[2] Y. Edan, K. Haghighi, R. Stroshine, and M. Cardenas-Weber, "Robot gripper analysis: finite element modeling and optimization," *Appl. Eng. Agric.*, vol. 8, no. 4, pp. 563–570, 1992.

[3] R. Kolluru, K. P. Valavanis, S. A. Smith, and N. Tsourveloudis, "Design fundamentals of a reconfigurable robotic gripper system," *IEEE Trans. Syst. Man, Cybern. Part ASystems Humans.*, vol. 30, no. 2, pp. 181–187, 2000.

[4] Y. Tlegenov, K. Telegenov, and A. Shintemirov, "An open-source 3D printed underactuated robotic gripper," in *Proc. 2014 IEEE/ASME 10th International Conference on Mechatronic and Embedded Systems and Applications (MESA)*, Sep. 2014, pp. 1–6.

[5] C. Vilau, N. Balc, D. Leordean, and C. Cosma, "Static analysis to redesign the gripper, using CREO parametric software tools," *Acad. J. Manuf. Eng.*, vol. 13, no. 1, pp. 77–82, 2015.

[6] S. Badadhe, A. P. Singh, S. Roy, and M. Tiwari, "Computer aided kinematic synthesis anddynamic analysis of robot end gripper mechanism," vol. 8, no. 10, pp. 30–45, 2018.

[7] S. Y. Qassab, H. A. Sultan, and S. O. Mohammad, "Modal analysis of pneumatic two finger robotic hand by finite element

analysis and experimental testing,"*Int. J. Eng. Technol. IJET-IJENS*, vol. 13, no. 03, 2011.

[8] G. R. Reddy and V. K. P. Eranki, Design and structural analysis of a robotic Arm. p. 101, 2016, [Online]. Available: http://www.divaportal.org/smash/get/diva2:1068547/FULLTEXT02

[9] K. B. Álvaro Meneses Martínez, "Mechanical design of a robot's gripper," Warsaw, 2015. [Online]. Available: https://1library.co/document/zpk68e0y-of-a-robot-s-gripper-mechanical-design.html

[10] M. Guo *et al.*, "Design of parallel-jaw gripper tip surfaces for robust grasping," in *Proc. 2017 IEEE International Conference on Robotics and Automation (ICRA)*, May 2017, pp. 2831–2838.

[11] M. A. González-Palacios, A. Silva-Caballero, M. A. González-Palacios, and L. A. Aguilera-Cortés, "Implementation of the Slide-O-Cam mechanism in the design of a robot gripper,"no. January,pp. 19–25,2011, [Online]. Available: https://www.researchgate.net/publication/268394255

[12] B. Doğan, "Development of a two-fingered and a four-fingered robotic gripper," Middle East Technical University, 2010. [Online]. Available: http://etd.lib.metu.edu.tr/upload/12611863/index.pdf

[13] V. A. Dheeraj and K. Rajagopal, "Material and cost analysis of five fingered robot gripper,"*IOSR J. Mech. Civ. Eng*, vol. 14, no. 4, pp. 37–42, 2017.

[14] J. Case and A. H. Chilver, *Strength of Materials: An Introduction to the Analysis of Stress and Strain*, Reprinted. Northern Ireland: EDWARD ARNOLD (PUBLISHERS) LTD, 1959.

[15] B. J. Schwarz and M. H. Richardson, "Introduction to operating deflection shapes,"*CSI Reliab. Week*,no. Vibrant Technology, Inc. Jamestown, California 95327,pp. 1–7,1999, [Online]. Available: https://www.semanticscholar.org/paper/INTRODUCTION-TO-OPERATING-DEFLECTION-SHAPES-By-Schwarz-Richardson/4c8953db113a0033c32a5ff89b99b7a6a503132b#paper-header

[16] N. Liu, D. L. Zou, T. J. Zhou, and J. W. Zhao, "Modal Analysis of Scraper Chain Industrial Robot System," *Appl. Mech. Mater.*, vol. 490–491, pp. 1190–1193, Jan. 2014.

[17] W. Ai and Q. Xu, "New structural design of a compliant gripper based on the Scott-Russell mechanism," *Int. J. Adv. Robot. Syst.*, vol. 11, no. 12, p. 192, Dec. 2014.

[18] S. Xiao, Y. Li, and X. Zhao, "Optimal design of a novel micro-gripper with completely parallel movement of gripping arms," *IEEE Conf. Robot. Autom. Mechatronics, RAM - Proc.*, pp. 35–40, 2011.

[19] X. Zhang and Q. Xu, "Design and analysis of a compound constant-force mechanism for compliant gripper,"*MARSS 2018 - Int. Conf. Manip. Autom. Robot. Small Scales*, no. Vcm, pp. 1–6, 2018.

[20] M. A. B. Marzuki, M. H. A. Halim, and A. R. N. Mohamed, "Determination of natural frequencies through modal and harmonic analysis of space frame race car chassis based on ANSYS," *Am. J. Eng. Appl. Sci.*, vol. 8, no. 4, pp. 538–548,2015.

[21] Y. H. Anis, W. L. Cleghorn, and J. K. Mills, "Modal analysis of microgrippers used in assembly of MEMS devices,"in *Proc. 2005 Int. Conf. MEMS, NANO Smart Syst. ICMENS 2005*, pp. 281–286, 2005.

[22] X. Zhang and Q. Xu, "Design and testing of a novel 2-DOF compound constant-force parallel gripper," *Precis. Eng.*, vol. 56, no. January, pp. 53–61, Mar. 2019.

[23] S. Sahu and B. B. Choudhury, "Stress and modal analysis of six-axis articulated robot using ANSYS," in *Lecture Notes in Networks and Systems*, vol. 40, Springer Singapore, 2019, pp. 303–311.

[24] A. H. Bhelsaikar, D. Roy, and V. Atpadkar, "Estimation of dynamic characteristics of a novel non-parallel detachable-jaw robotic gripper using finite element method," *J. Phys. Conf. Ser.*, vol. 1831, no. 1, 2021.



**Ahmed Khalid Ahmed** was born on January 4, 1985, and received his BSc in Electrical Engineering (2006) and MSc in Mechatronics (2012) from Salahadin University, Iraq - Erbil. He is also currently pursuing his Ph.D. degree at the same university. In addition, he is an assistant lecturer at the Department of Electrical Engineering / College of Engineering - Salahadin University-Erbil. His research areas include robotics, industrial robots, Mechatronics systems, Control Engineering, Automation Systems, Additive Manufacturing, Microcontroller Programming, Digital Electronics, Embedded Electronics, PC Interfacing, Robot Control, Manipulator Robots, Manipulator Robots Dynamics, Mobile Robotics, DASYLab - Data Acquisition Systems, Fusion 360 CAD/CAM/CAD software.

**Safeen Yaseen Ezdeen** was born on 1961 in Erbil, Iraq. He received a B.Sc. degree in Mechanical Engineering and M.Sc. degree in Applied Mechanic from Technology University-Baghdad, Iraq, in 1984 and 1990, respectively, and a Ph.D. degree in Design from the University of Baghdad in 2001.

Dr. Safeen is a lecturer in the Mechanical Engineering Department, College of Engineering - Salahadin University -Erbil, Iraq. In February 2009, he got Professor's Degree, and from 2012 to 2017, he was the Dean of the College of Engineering. He published around 27 papers in local and ISI journals and conferences. Furthermore, He is an Editorial and reviewer Board for different International Journals. His research and work interests are the Design of satellites, Vibration, Control, Stress Analysis, and Finite element Methods.

**Ahmad Mohamad Sinjari** was born in Sinjar, Iraq. He received a B.Sc. degree in Electrical Engineering from Salahadin University Erbil-Iraq in 1987. Additionally, he earned a Master of Science in Microprocessor technologies in distance measuring protection from Mosul University-Mosul, Iraq, in 1993, and a Ph.D. in MEMS technology in automotive radars from the University of Windsor-Canada in 2010.

Dr. Ahmad is a lecturer in the Electrical Engineering Department, College of Engineering - Salahadin University -Erbil, Iraq. He published 9 US patents and 11 papers in local and ISI journals and conferences. Furthermore, He got more than 30 years in the automotive industry and academics. His research areas include MEMS technology, PLC, industrial robots, UPPAAL, and Automation Systems.